arXiv:2512.19691v1 [cs.AI] 22 Dec 2025

Scalably Enhancing the Clinical Validity of a Task Benchmark with Physician Oversight

Junze (Tony) Ye[1], BS; Daniel Tawfik[2], MD, MS; Alex J. Goodell[3], MD, MS; Nikhil V. Kotha[4], MD; Mark K. Buyyounouski[4], MD, MS; Mohsen Bayati[1,4,5], PhD

[1]Department of Operations, Information and Technology, Stanford Graduate School of Business, Stanford, CA
[2]Department of Pediatrics, Division of Critical Care Medicine, Stanford University School of Medicine, Stanford, CA
[3]Department of Anesthesiology, Perioperative and Pain Medicine, Stanford University School of Medicine, Stanford, CA
[4]Department of Radiation Oncology, Stanford University School of Medicine, Stanford, CA
[5]Department of Electrical Engineering, Stanford University School of Engineering, Stanford, CA

Automating clinical risk-score computation promises to reduce administrative burden, but rigorous evaluation requires benchmarks whose labels reflect clinical ground truth. Increasingly, such benchmarks are constructed with partial LLM assistance (e.g., feature extraction and code-based aggregation), which means the resulting "gold" labels can encode historical model and tooling errors. Treating these artifacts as static oracles is especially hazardous when they are reused as reward signals for reinforcement learning (RL), where label noise becomes a teacher rather than a yardstick. We propose viewing complex clinical workflow benchmarks as living documents that require periodic, transparent re-auditing and clinician-guided maintenance. We introduce a scalable physician-in-the-loop maintenance pipeline that combines agentic LLM verifiers with automated triage to concentrate scarce clinician attention on the most contentious instances. In a case study on the original MedCalc-Bench release, our audit and independent recomputation identify a substantial fraction of test labels that diverge from medical ground truth due to extraction errors, calculator logic mismatches, and task underspecification (including clinically unanswerable cases). Physician single-blind review indicates higher agreement for the maintained labels. Finally, in a controlled GRPO fine-tuning experiment on Qwen3-8B, changing only the reward labels yields an 8.7% absolute improvement in test accuracy when evaluated against physician-aligned labels, demonstrating that benchmark maintenance materially affects downstream alignment. Together, these results argue that in safety-critical domains, benchmark stewardship—auditing, versioning, and clinician oversight, is prerequisite infrastructure for reliable model evaluation and training.

Key words: Generative AI, AI alignment, medical decision making, reinforcement learning, expert elicitation, data quality

1. Introduction

A clinician's daily workflow is fundamentally an exercise in resource allocation, split between high-value complex clinical judgment and repetitive administrative tasks involving the retrieval and synthesis of fragmented data from the Electronic Health Record (EHR). This clerical burden creates a significant operational bottleneck; it is a primary driver of physician burnout, which has been linked to significant patient safety risks and estimated costs to the U.S. healthcare system reaching

billions of dollars annually (Han et al., 2019; Sinsky et al., 2022; Muir et al., 2022; Tawfik et al., 2024). Integrating technology to optimize these workflows and alleviate cognitive load has shown promise in improving clinician well-being, operational efficiency, and clinical outcomes. In particular, the advent of Large Language Models (LLMs) has opened new avenues for such enhancement, ranging from ambient AI scribes that reduce documentation time (Tierney et al., 2024, 2025) to "copilots" that verify medication prescriptions (Pais et al., 2024) or selectively trigger safety alerts in live care (Korom et al., 2025).

In this paper, we focus on one such high-frequency administrative task: the calculation of standardized medical risk and stratification scores. These calculations are ubiquitous in hospital settings, for instance, determining pneumonia severity (CURB-65) upon a patient's arrival at an Emergency Department, or assessing stroke risk (CHA_2DS_2-VASc) to guide anticoagulation therapy (Lim et al., 2003; Lip et al., 2010). These metrics synthesize patient history, vitals, and laboratory results into actionable scalars that directly inform high-stakes operational decisions: prioritizing patient flow in triage, determining the appropriate level of care (e.g., admission planning), and applying preventative interventions (prophylaxis).

Traditionally, these scores are computed manually: a clinician reads the EHR, extracts the necessary criteria, and inputs them into a bedside calculator such as MDCalc, a web app that has between three and five million visits per month and is used by 65% of physicians in the US (MDCalc, 2024). However, the manual extraction of clinical criteria from unstructured notes is time-consuming and prone to mistakes. The emergence of LLMs offers a transformative vision: automated systems that can read EHR notes, extract relevant clinical features, and reliably compute these scores end to end (Xie et al., 2024a; Goodell et al., 2025; Jin et al., 2025; Wang et al., 2025b; Roeschl et al., 2025). But as we move toward deploying or even researching such systems, a fundamental question of quality assurance arises: *how do we ensure these automated systems are computing the "right" scores, specifically, scores that align with the ground truth judgment of a licensed physician*?

To answer this question, the research community requires an accessible evaluation standard. In this domain, *MedCalc-Bench* (Khandekar et al., 2024) stands as a foundational contribution. By curating de-identified patient notes from PubMed Central and mapping them to 55 widely calculated medical scores on MDCalc web app, Khandekar et al. (2024) established the first large-scale public testbed, involving 11,000 samples, for end-to-end clinical score computation. To generate labels at scale, the authors employed a two-stage pipeline: using GPT-4 to extract clinical features from text, followed by Python scripts to aggregate those features into final scores. This effort provided the field with a standardized definition of the task and a shared dataset, enabling subsequent research to benchmark progress in medical reasoning (Oh et al., 2025; Liu et al., 2025a). Consequently, the

labels provided by MedCalc-Bench have effectively become the ground truth against which new models are evaluated and, increasingly, the target distribution on which they are trained.

However, the reliance on largely LLM-generated "gold standard" labels introduces a unique systemic risk: these labels inherently echo the model's capabilities and flaws at the time of creation. The original MedCalc-Bench labels relied on the extraction capabilities of GPT-4 in early 2024 and the assumption that programmed calculators perfectly mirror clinical intent. When such a benchmark is treated as a static oracle, errors in the original extraction or calculator logic become enshrined as systemic biases in the evaluation signal. This creates a dangerous feedback loop, particularly when benchmarks transition from evaluation sets to training signals. In modern Reinforcement Learning (RL) setups (Ahmadian et al., 2024), inaccurate labels are not just a mislabeled yardstick, but a biased teacher that actively steers models away from clinical reality.

While benchmarks have been instrumental in accelerating progress, this challenge of latent inaccuracies necessitates a more rigorous approach to their lifecycle, grounded in principles of continuous quality control. We argue that LLM-assisted benchmarks for complex clinical workflows are not static measurement instruments; they are socio-technical artifacts whose labels inherit the failure modes of the models, tools, and procedural assumptions used at the time of creation. They should therefore be treated as *living documents* with explicit maintenance practices (auditing, clinician adjudication, versioning, and documentation). We do not position our improved labels as a definitive replacement for MedCalc-Bench; rather, we use the original release as a case study to motivate transparent, repeatable benchmark stewardship and to quantify how label fragility affects downstream model development.

In this work, we approach benchmark maintenance not as an ad-hoc error correction task, but as an optimized quality assurance process. We design a systematic, replicable collaboration between advanced agentic LLMs (as verifiers) and human physicians, focused on the central operational constraint: scarcity of expert attention. Our approach proceeds in three steps: (1) an automated audit where an LLM verifier flags potential errors in the original labels; (2) an independent maintenance pipeline that recomputes scores from scratch to identify systematic divergences; and (3) a targeted physician adjudication of divergent cases. In short, we leverage agentic AI to scale re-auditing and triage, thereby concentrating scarce clinician time on the most consequential disagreements.

The above approach shows that a non-trivial fraction of the original labels diverge from physician judgment due to feature extraction errors, calculator logic mismatches, or clinical ambiguity (e.g., unanswerable questions). Furthermore, we demonstrate the downstream impact of unmaintained labels through a controlled LLM fine-tuning experiment. By fine-tuning a Qwen3-8B model (Qwen, 2025) via Group Relative Policy Optimization (GRPO) (Shao et al., 2024), a commonly used RL algorithm, we show that changing only the reward labels (original versus maintained) yields an

8.7% absolute difference in test accuracy when evaluated against physician-aligned labels. The goal of this experiment is not to claim superior benchmark performance; rather, it is to test whether label noise materially impacts trained model accuracy, a meaningful question because one plausible outcome was that the noise would be "washed out" by the strength of signal in the data. Our results indicate otherwise, confirming that benchmark maintenance has tangible consequences for downstream alignment.

Our contributions are summarized as follows:

- **Modeling the label generation process.** We mathematically model the data generating process underlying the original MedCalc-Bench gold labels (§2.1). This abstraction allows us to attribute how procedural errors in extraction and aggregation distort the ground truth estimate. Furthermore, we extend this model to the alignment phase, formalizing how label noise propagates into the reward function of the Markov Decision Process (MDP) used in RL training (§4.1).
- **Operationalizing benchmark stewardship.** We design and implement a physician-in-the-loop system that operationalizes scalable oversight by optimizing the allocation of expert attention. By aggregating evidence from two independent, agentic LLM pipelines, the system triages the most contentious instances in MedCalc-Bench for targeted physician expert review (§3.1, 3.2). In a single-blind validation sample, the resulting maintained labels exhibit higher agreement with physician judgment (§3.2.1)[1].
- **Quantifying the impact on LLM alignment.** Using a controlled RL experiment on a modern open-source LLM, we quantify how different label choices (original versus maintained) become training rewards that significantly impact LLM alignment (§4). This analysis highlights that label fragility in an LLM-assisted benchmark can simultaneously distort model behavior and the metrics by which that behavior is perceived by its human trainers.

1.1. Literature Review

Integrating LLMs into clinical workflows. LLM-based systems are increasingly embedded in routine care for documentation, medication safety, and clinical decision support. At health-system scale, ambient AI scribes have been deployed to draft visit notes inside the EHR and are associated with reduced documentation burden and high clinician adoption (Tierney et al., 2024, 2025). For medication safety, Pais et al. (2024) develop an LLM-based "copilot" that reduces prescription direction-related errors and increases automation in an online pharmacy. In quantitative decision support, Goodell et al. (2025) show that tool-augmented LLM agents can reliably call vetted clinical calculators, while Khandekar et al. (2024) demonstrates that general-purpose LLMs still struggle

[1] Most raw results and intermediate data are published in https://github.com/junzeye/validate-medcalc-labels; we will update the repository with processed code and data artifacts as curation and formatting is completed.

with end-to-end medical calculations even when their explanations are fluent. Beyond calculators, Korom et al. (2025) evaluate an LLM-based safety net integrated into a real EHR system in a large field study, and find that selectively triggered alerts reduce clinician-rated diagnostic and treatment errors in live care. These systems motivate our focus on MedCalc-style calculators as a concrete use case where LLM systems and domain-specific evaluations need to be co-designed.

Healthcare cost of burnout. A larger problem we hope to solve is the reduction of clerical burdens and its cost for the U.S. healthcare system. Clinician burnout carries substantial economic consequences: Han et al. (2019) and Sinsky et al. (2022) both estimate excess annual U.S. healthcare expenditures attributable to physician turnover to be in the billion USD scale, with a sizable share specific to burnout-related turnover, while Muir et al. (2022) show that nurse burnout-attributed turnover substantially increases hospital costs in a Markov modeling analysis. Tawfik et al. (2024, 2025) show a correlation between EHR-related work burden and primary care physician burnout. These results underpin the motivation for clerical support tools such as ambient AI scribes and for our narrower focus on automating repetitive, text-based decision support as one contributor to documentation and cognitive load.

Data-driven decision making. Our framework views benchmark maintenance not merely as curation, but as an operational decision process, allocating scarce physician time to maximize data quality. This perspective connects our work to the extensive literature on data-driven decision making in operations. While a comprehensive review of this vast field is beyond our scope, we briefly discuss two paradigms.

The first is the "predict-then-optimize" paradigm: one first estimates uncertain outcomes from historical data and then solves a stochastic or robust optimization problem treating these estimates as inputs. Representative examples include (Bertsimas and Thiele, 2006; Delage and Ye, 2010; Bayati et al., 2014; Ferreira et al., 2016; Acimovic and Graves, 2015). While this two-stage architecture has enabled large-scale deployments, it can be inefficient when predictive error is misaligned with the downstream decision objective. Motivated by this, the prescriptive analytics literature proposes to learn mappings from covariates directly to decisions (Liyanage and Shanthikumar, 2005; Bertsimas and Kallus, 2020; Ban and Rudin, 2019; Elmachtoub and Grigas, 2022).

A second complementary stream focuses on policy learning and sequential experimentation. Building on early work on treatment choice under ambiguity (Manski, 2004), methods such as outcome-weighted learning (Zhao et al., 2012) and empirical welfare maximization (Kitagawa and Tetenov, 2018; Athey and Wager, 2021) use data to learn policies with provable guarantees (Aswani et al., 2019). Furthermore, when information accrues over time, bandit algorithms provide a paradigm for adaptive decision making, ranging from classical index policies (Katehakis and Veinott, 1987; Chick and Gans, 2009) to contextual bandits in healthcare (Bertsimas and Mersereau,

2007; Besbes and Zeevi, 2009; den Boer and Zwart, 2014; Harrison et al., 2012; Bastani and Bayati, 2020).

Our work connects broadly to this literature through its machine learning model training and validation. Similar to how data-driven operations seek to validate and optimize decision rules, we focus on generating a high-quality test set to evaluate an agent's performance and utilizing RL to update its training policy. However, our main objective is to apply these methods to the *alignment* of the AI model itself, ensuring that the ground-truth signals used for both evaluation and training accurately reflect expert clinical judgment.

Concurrent Work. Wang et al. (2025a) also reexamines MedCalc-Bench, introducing an LLM-judged, stepwise evaluation framework to provide process-level rewards at test time; they additionally exclude about 10% of the original test set but otherwise treat the remaining labels as fixed. Our work is complementary: we develop a physician-in-the-loop maintenance pipeline that combines two independent agentic LLM auditing processes with targeted clinician adjudication, ultimately flagging over one quarter of test instances as likely label errors. While their approach enhances diagnostic granularity at test time, it introduces a dependency on the judging model's capabilities and biases at each step, which may compound in the aggregated final reward. In contrast, our work focuses on upstream benchmark stewardship, auditing, triage, and clinician adjudication of the labels that define both evaluation targets and RL rewards. We further show that training an RL-aligned model on maintained versus original labels leads to a sizable change in test accuracy, underscoring the operational importance of reward-label choice. In parallel, the MedCalc authors released an updated MedCalc-Bench v1.2 on HuggingFace; ongoing revisions by benchmark creators are expected and healthy, and our results are intended to motivate transparent revision methodology and routine re-auditing. All audits and maintenance in this paper are conducted on the original NeurIPS release,[2]. Lastly, Roeschl et al. (2025) recently report that when computing cardiovascular scores, a hybrid pipeline separating LLM-based data extraction from rule-based score calculations surpasses the accuracy of scores computed by physicians on the fly.

2. Medical Score Computing and its Ground Truth Labeling

In this paper, "task" and "workflow" are two related but different concepts. A *task*, we say, is a directive to obtain a verifiable outcome when given an input, without specifying the ideal problem-solving procedure. Given a task, a *workflow* is the operational process which an agent can execute to complete the task. In the following, we mathematically abstract how medical computing workflows are often operationalized in practice, and explain the state-of-the-art public benchmark environment for evaluating an LLM agent's capability on medical computing tasks.

[2] https://huggingface.co/datasets/ncbi/MedCalc-Bench-v1.0, Commit ID: `4f75ddac6f87fde2cff438a7a971ac987040d5af`, updated on Nov 12th, 2025; the URL to the original .csv file, which we accessed in June 2025, is now unavailable.

Table 1 Mapping Formalism to a Concrete Example: The LACE Score

Mathematical	Formal	LACE Score for Readmission
C	Patient context (EHR notes and lab data)	*"72M admitted to ED for CHF exacerbation. Hospital stay was 4 days. Hx of diabetes (CCI=2). Visited the ED twice in last 5 months."*
q	Medical score to compute	*"What is the patient's LACE score?"*
$(q_i)_{i=1}^m$	Sub-questions for each feature	q_1: Patient's **L**ength of stay? q_2: **A**cuity of admission? q_3: **C**harlson Comorbidity Index? q_4: # **E**D visits in last 6 months?
$f_\theta(C, q_i)$	**Stage 1:** Feature extractor (language processing)	Clinician/LLM reads C to find answers to each q_i
$\boldsymbol{x} \triangleq (x_i)_{i=1}^m$	Clinical features vector, where $m = 4$ for LACE	$x_1 =$ 4 days ($\in \mathbb{R}$) $x_2 =$ Emergent ($\in \mathcal{C}$) $x_3 =$ CCI score of 2 ($\in \mathbb{R}$) $x_4 =$ 2 visits ($\in \mathbb{R}$)
$g_\phi(x_1, ..., x_m)$	**Stage 2:** Aggregation function (rule-based reduction)	Rule ϕ: Map to points then sum 4 days $\rightarrow$ 4pts, Emergent $\rightarrow$ 3pts CCI 2 $\rightarrow$ 2pts, 2 visits $\rightarrow$ 2pts $g_\phi = 4 + 3 + 2 + 2 = \mathbf{11}$
y	Final computed score	**11**
$G_{\phi,\theta}[C, q]$	End-to-end pipeline composition	Raw EHR note $\rightarrow$ Extract 4 features $\rightarrow$ Apply LACE rules $\rightarrow$ **Score = 11**

2.1. Mathematical Formalism

A typical workflow of computing a medical score can be decomposed into two stages: (1) evaluating a fixed set of score-specific clinical features (a.k.a. clinical criteria) based on the patient's medical history, then (2) formulaically aggregating the feature values into a scalar score, either by hand or a custom calculator app like MDCalc. In symbols, we may denote the patient context (natural language texts interleaved with tabular lab data) by C and a description of the medical score to compute by q. The feature vector typically used to answer q can be denoted by $\boldsymbol{x} \triangleq (x_i)_{i=1}^m$ where $m \in \mathbb{N}$ is uniquely determined by q. $(x_i)_{i=1}^m$ can be thought of as answers to $(q_i)_{i=1}^m$ where q_i is a sub-question of q, described in natural language, that a clinician or LLM needs to answer. For each i, the per-feature domain $\mathcal{X}_i$ contains the following:

1. real numbers, e.g. blood pressure, Likert scale response;
2. categorical values, ranging from True/False to symptom groups—we call this a set $\mathcal{C}$;
3. a fallback undefined token denoted by NA, indicating unextractability of a feature.

In sum, $x_i \in \mathcal{X}_i := \mathbb{R} \cup \mathcal{C} \cup \{\mathsf{NA}\}$. Let $\boldsymbol{\mathcal{X}} \triangleq \prod_{i=1}^m \mathcal{X}_i$ denote the feature space, a Cartesian product of individual per-feature domains. Lastly, for each (C, q) let y be *any* answer predicted by an algorithm,

and y^* be the (latent) clinically correct ground truth answer; y^* is a scalar if the question q is answerable given C, and NA if C lacks crucial information or is not clinically suited for answering q. Perfectly observing y^* is costly, so an estimator $\hat{y}$ ($\hat{y}_{\mathsf{original}}$ for MedCalc-Bench, $\hat{y}_{\mathsf{new}}$ for ours) is used.

Stage (1): Extracting Features. With the above notations, and let $\mathcal{T}$ be the set of all displayable computer texts. The first stage of the workflow is abstracted as applying a highly flexible language processing function $f_\theta : \mathcal{T} \to \bigcup_i \mathcal{X}_i$ for each one of $x_i = f_\theta(C, q_i)$ for $1 \le i \le m$, i.e., m times applying f_θ. The language processor f_θ is traditionally instantiated by a human healthcare provider who reads patient EHR notes to determine the q_i's, but nowadays the rise of generative AI makes it possible to augment human-only processing with LLM auto-completions.

Stage (2): Aggregating Features. Given the feature vector $\boldsymbol{x}$ extracted in Stage (1), the second stage applies a rule-based, deterministic reduction operator g_ϕ (Of course, g_ϕ is specific to each score question q, but for notational simplicity, we do not include q in the notation) that maps the feature tuple $(x_i)_{i=1}^m$ to a scalar output $y \in \mathcal{Y}$. The parameter ϕ represents the score-specific rule, e.g. arithmetic formula, look-up table, or piecewise-defined condition, that defines how the features jointly contribute to the final score. Formally:

$$g_\phi : \boldsymbol{\mathcal{X}} \mapsto \mathcal{Y}, \quad y = g_\phi(\boldsymbol{x}) = g_\phi(x_1, ..., x_m)$$

where $\mathcal{Y} \subseteq \mathbb{R} \cup \{\mathsf{NA}\}$ is the space of possible score values. If at least one feature in $\boldsymbol{x}$ is out-of-range or NA, the final score is not computable and NA is returned.

Putting the two stages together, we can visualize the overall workflow of computing a medical score as a compositional pipeline:

$$(C, q) \xrightarrow[\text{extracts}]{f_\theta} (x_1, x_2, \ldots, x_m) \xrightarrow[\text{aggregates}]{g_\phi} y.$$

The end-to-end pipeline can be abstracted by a composed function $G_{\phi,\theta}[C, q] : \mathcal{T} \mapsto \mathcal{Y}$, specifically

$$G_{\phi,\theta}[C, q] \triangleq g_\phi(f_\theta(C, q_1), \ldots, f_\theta(C, q_m)).$$

Remark 2.1 (Insights from the Formalism). The above formalism abstracts the *sequential modularity* of a typical medical computing workflow and the *graphical structure* of information flows: the first stage (f_θ) interprets and extracts structured intermediate variables from unstructured data, while the second stage (g_ϕ) performs a rule-based routine to aggregate the intermediate bits into a clinically verifiable and actionable scalar output. Of course, not all end-to-end workflows follow this specific pipeline structure; a system designer may as well eliminate g_ϕ and use a single call of f_θ to directly output the scalar output. That said, Khandekar et al. (2024) employed the former, structured data generation approach, so understanding this allows us to attribute any deviation in the final output y to a parameter extraction error in f_θ, or a formulaic mistake in g_ϕ, or both.

2.2. Current task evaluation standard

To our best knowledge, the only large-scale public benchmark dataset for evaluating an agentic system's end-to-end score computing capability is MedCalc-Bench (Khandekar et al., 2024), created and released by researchers at NIH/NLM and five US medical schools. Their benchmark task asks an LLM model to read a patient note and answer a medical score computation question, and the model's final answer y is graded correct if it is within a $\pm 5\%$ margin of a gold label value $\hat{y}_{\text{original}}$ that the benchmark authors synthesized; and in cases where y should be a datetime, exact string match is required. A model's performance is quantified as the average accuracy on the benchmark's test data set, which are 1047 instances manually reviewed by those authors.

MedCalc-Bench authors curated the benchmark data and labels in the following manner:

1. Patient notes are real, deidentified patient cases they scraped from journal-published medical papers that are archived in the PubMed Central database. There are altogether 10,053 + 1,047 = 11,100 notes in the train and test sets. We note that each of these patient notes can be seen as a unique context C in the notation of §2.1.

2. The medical score questions (q's), e.g. "What is the patient's Glasgow Coma Score?", are sourced as the 55 unique calculators listed as "popular" on MDCalc.com, a web app widely used by U.S. physicians. One can think of each train or test instance in the MedCalc-Bench dataset as uniquely identified by a pair (C, q). Many instances may share the same score question q, though their patient context C will differ.

3. $\hat{y}_{\text{original}} \in \mathcal{Y}$, MedCalc-Bench's ground truth label of each (C, q), was synthesized in a procedure analogous to the compositional pipeline we presented in 2.1. They used `GPT-4` as f_θ and themselves hard-coded the logic of g_ϕ of each unique q individually as 55 Python scripts.

Table 2 Some Reported MedCalc-Bench results.

Paper	Base Model	Setup	Acc.
Khandekar et al. (2024)	GPT-4	one-shot	50.9
Oh et al. (2025)	Llama3-70B	4-bit quantized	40.0
Wang et al. (2025a)	GPT-4o	RAG + code	59.6*
Liu et al. (2025a)	GPT-4o	multi-agent + tool use	67.7
Zhang et al. (2025)	Qwen2.5-7B	RLVR	57.6
Lin et al. (2025)	DeepSeek-R1	zero-shot	48.1
Lin et al. (2025)	Llama3-3B	SFT + RLVR	52.0

"Acc." is overall accuracy on the test set (%) of MedCalc-Bench. "Setup" refers to each study's main adaptation technique of the base model. All studies reported using Chain-of-Thought (reasoning mode) in their LLM inference.
*This reported result was evaluated on a subset of the original MedCalc test set (940/1047).

Since June 2024, multiple academic studies have used MedCalc-Bench as an evaluation benchmark or finetuned open-weight models on its train set. Table 2 shows a partial anthology of some test

accuracies recently reported. Several survey papers on LLM and healthcare, including Xie et al. (2024b); Zhou et al. (2025); Xu and Sankar (2025), cited this benchmark. It is also included in the test suite of MedHELM (Bedi et al., 2025), a comprehensive framework for evaluating medical LLMs. These references indicate that MedCalc-Bench is an influential benchmark in the field.

2.3. Concerns about MedCalc's Original Labeling Approach

MedCalc-Bench represents a significant contribution to evaluating AI for healthcare workflows. By sourcing real, de-identified patient notes and pairing them with 55 popular calculation tasks from MDCalc.com, the benchmark provides a far more realistic simulation of clinical tasks than traditional multiple-choice question answering. This curation represents a substantial effort by the authors to balance patient privacy with the need for accessible, high-quality evaluation data.

However, we have concerns about the procedure through which MedCalc-Bench synthesized the ground truth values $\hat{y}_{\mathsf{original}}$'s, particularly regarding the reliability of their chosen f_θ and g_ϕ. First, for both the train and test sets, the MedCalc authors used GPT4 as their feature extractor (f_θ) to produce the clinical features vector $\boldsymbol{x}$, instructing it to output a JSON dictionary directly without intermediate reasoning. Although the authors reported manually checking this parameter extraction, their paper provides no statistics on the level of disagreement between their human reviewers and the GPT4-extracted values. Such disagreement seems probable, especially given that earlier versions of GPT4 were more prone to factual hallucinations than contemporary models.

Second, the level of alignment between their 55 Python functions (their g_ϕ) and the formulas used by MDCalc.com is unclear. Given that MDCalc.com is used daily by many US physicians, its formulas represent a de facto standard. The authors did not detail the derivation process for their Python scripts, making it difficult to know if they were all fact-checked by licensed physicians.

As explained in Remark 2.1, each of these potential discrepancies in f_θ and g_ϕ could contribute to an accumulation of error in the final gold label. This motivates our work in §3 to systematically examine the true label quality of the benchmark.

Remark 2.2 (Aligning Ground Truth Labels). If ground truth y^* were to be thought of as a point value and $\hat{y}$ be a benchmark's estimate of it, the alignment objective could be loosely interpreted as minimizing the estimator bias $B(\hat{y}) := \mathbb{E}_{\hat{y}\sim D(\theta,\phi)}[\hat{y}] - y^*$, where $D(\theta, \phi)$ emphasizes the sampling distribution's dependence on both on the LLM weights θ and the rule-based aggregation logic ϕ stipulated by the human researcher. If there is high heterogeneity in how human clinicians themselves interpret a clinical criterion (low inter-rater reliability), y^* might be better modeled as a distribution; and the alignment objective be approximated as minimizing some statistical distance, e.g. KL divergence or Wasserstein distance, between y^* and $\hat{y}$. In this paper, we adopt the former, point-estimate view of y^* with a $\pm 5\%$ margin for real-valued outputs, reflecting the evaluation guideline given by MedCalc-Bench. That said, we want to acknowledge the possible suitability of the second approach for certain medical score questions.

3. Systematic Alignment of MedCalc Benchmark Labels

To address reliability concerns identified in §2.3 regarding the benchmark's original labels, this section establishes a systematic framework for evaluating and improving label alignment with clinical knowledge. We organize our approach into two phases. In Phase 1 (§3.1), we conduct a scalable automated audit of the existing test set using a `Gemini-2.5-Pro` agentic pipeline, validated by a small-scale clinician review, to quantify the prevalence of label errors. Motivated by results uncovered in this audit, Phase 2 (§3.2) details a comprehensive relabeling workflow where we independently derive corrected ground truth values and then collect clinician feedback to quantify and compare the clinical alignedness of $\hat{y}_{\text{original}}$'s and $\hat{y}_{\text{new}}$'s.

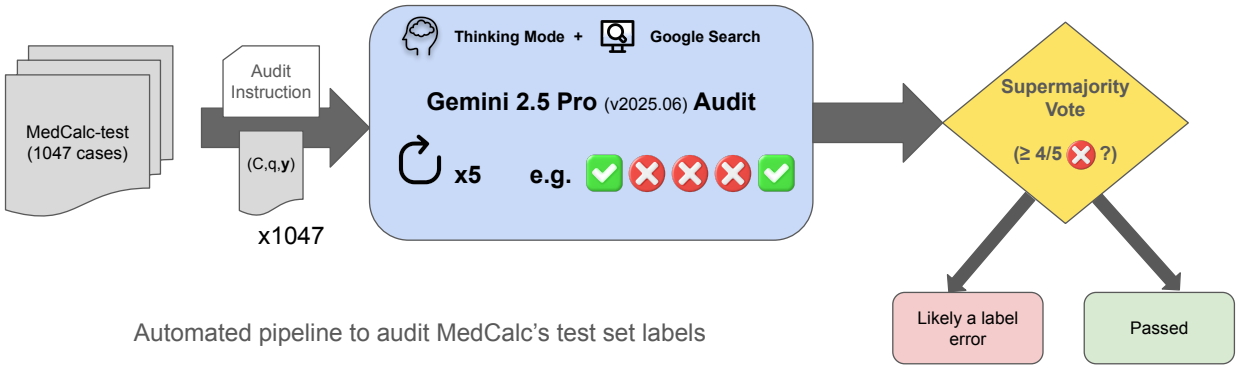

Figure 1 **In Phase 1, Gemini is endowed with Google search to individually validate 1047 $(C, q, \boldsymbol{y})$ instances provided in the original MedCalc-Bench release. After thinking and tool call(s), Gemini is instructed to give a binary judgment of if $\hat{y}_{\text{original}}$ is correct; the Gemini agent is queried 5 times, and we only count a case as problematic if there is supermajority agreement in the 5 responses. Note: $\boldsymbol{y} := (\mathcal{M}, \hat{y}_{\text{original}})$, where $\mathcal{M}$ is metadata (GPT4-extracted features x & text description of g_ϕ) MedCalc-Bench provided for how $\hat{y}_{\text{original}}$ was derived.**

3.1. Phase 1: Auditing Test Labels

Our pilot study focused on checking the label correctness of MedCalc's test set, as this is the subset ultimately used to benchmark an LLM's capability. The audit pipeline's backbone uses the June 2025 version of `Gemini-2.5-Pro` (Comanici et al., 2025), which was one of the most advanced reasoning LLMs when we conducted the audit in July and August 2025. Figure 1 summarizes the structure of the audit pipeline. In words, Gemini is applied five times separately to clinically validate how the MedCalc label $\hat{y}_{\text{original}}$ was originally derived for each and every (C, q), and we improve factual grounding by giving Gemini the ability to issue and reason on multiple Google search queries, rather than relying on its parametric knowledge. The reason for five applications of Gemini is to increase reliability, given the stochastic nature of LLMs generation. The overall pipeline

design is partly motivated by the *generation-verification gap* (Song et al., 2025); we believe that `Gemini-2.5-Pro`, enhanced with the said agentic abilities, serves as a strong verifier for outputs previously generated by a non-reasoning LLM in a single-turn, closed-book fashion (e.g. clinical features $\boldsymbol{x}$ extracted by `GPT-4`, or Python scripts codifying the g_ϕ's). Lastly, to reduce false positives, our system prompt asks Gemini to be conservative and only flag a test case as problematic if Gemini finds $\hat{y}_{\text{original}}$ to be incorrect in a clinically significant way. We provide the system prompt text and an example user prompt in the Appendix (Fig. 6).

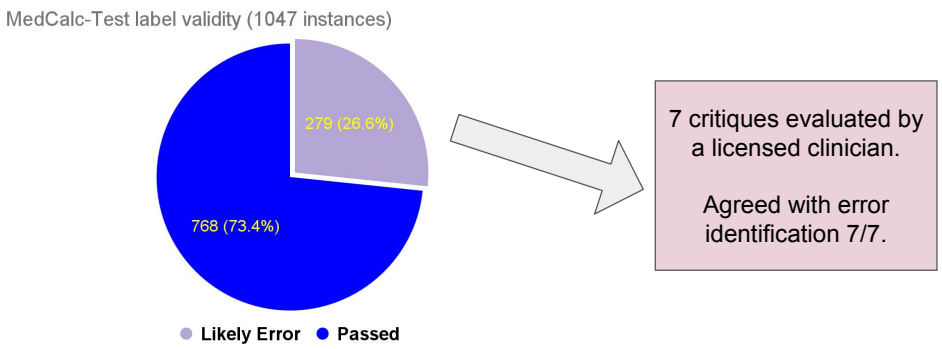

Figure 2 Phase 1 audit outcomes. 26.6% of MedCalc's test instances are flagged as `Likely Error`'s by the Fig. 1 pipeline. A pilot clinician spot-check (7 flagged instances) agreed with the audit feedback in 7/7 instances, giving an early signal of the audit pipeline's clinical validity.

3.1.1. Phase 1 Results

Automated audit outcomes. Running the pipeline on the full MedCalc test set ($n = 1{,}047$) surfaced a non-trivial number of label ($\hat{y}_o^*$) issues. In total, labels of 279/1,047 test instances (26.6%) were flagged as *Likely Error* by the verifier, while 768/1,047 (73.4%) passed (Fig. 2). Potential issues were distributed broadly across the distinct questions q (55 calculators popular on MDCalc): in 40 of the 55, at least one associated test instance (C, q) was flagged as a *Likely Error*. Since we only count an instance as *Likely Error* if $\geq 4/5$ independently sampled verifier runs all flag it, the statistics likely understate the true rate of controversial labels.

Physician expert feedback. As a reality check on the Gemini auditor's clinical judgment, a licensed physician independently selected and reviewed seven *Likely Error* instances related to his clinical specialty. For each instance, the physician read both $(C, q, \boldsymbol{y})$ and the Gemini auditor's critique of $\boldsymbol{y}$. He agreed with the critiques in all 7/7 reviews. While the sample size is modest, this reality check supports the viability of using a reasoning LLM with tool use for label auditing.

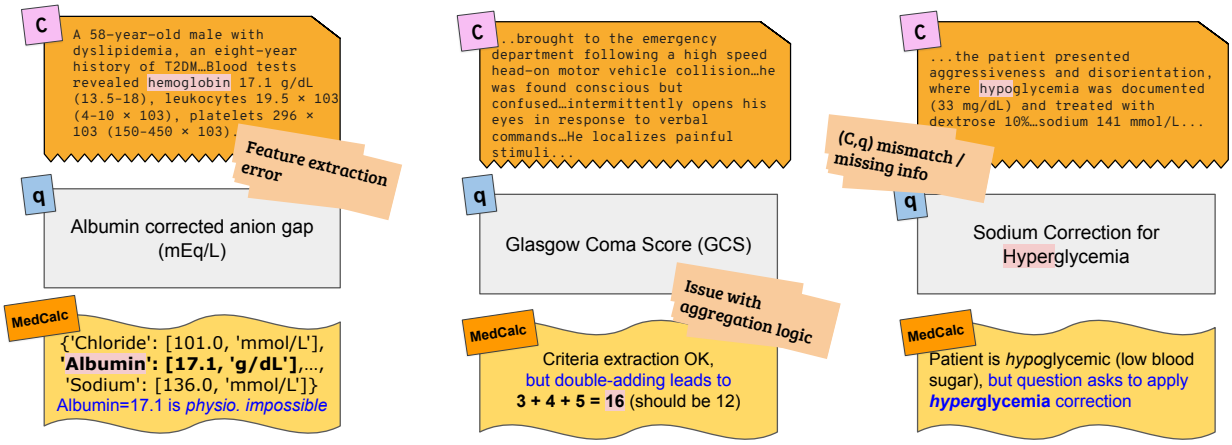

Figure 3 Representative error types. (a) Feature extraction error, i.e. f_θ extracted a feature x_i incorrectly: GPT-4 might have confused "hemoglobin" with "albumin", scrapping a value that is physiologically impossible and biasing $\hat{y}_{\text{original}}$; (b) Incorrect aggregation logic (g_ϕ): a Glasgow Coma Scale aggregation code that double-adds a feature value; (c) q is not answerable given C (mismatch / missing information): a Sodium correction for hyperglycemia applied to a clearly hypoglycemic patient. Row IDs for 3 examples in `test.csv`: 772, 849, 374.

Qualitative error taxonomy. Manual inspection of flagged instances reveals three recurring failure modes in the original ground truth derivation: (a) **feature extraction errors** (flawed f_θ), (b) **incorrect aggregation logic** (flawed g_ϕ), and (c) q **is not answerable given** C. Figure 3 illustrates one example of each. In these modes, (a) and (b) map directly onto the two-stage formalism in §2.1, whereas (c) correspond to either $f_\theta(C, q) = \text{NA}$ or $g_\phi(\boldsymbol{x}) = \text{NA}$. In the case of (c), it would be more reasonable to reward the LLM for *abstaining* from answering the impossible and responding with NA ("Not Available"), instead of hallucinating an answer. Moreover, instead of throwing away all these instances, we suggest that the benchmark recycle these them by keeping (C, q) but revising the ground truth label from $\hat{y}_{\text{original}}$ to NA. Correspondingly, the benchmark's inference prompt could acknowledge that there are instances where the correct answer is to abstain. A safely useful LLM system, we believe, should act as a triage agent that seeks human review for out-of-distribution (C, q) instances, while strictly limiting abstention on normal cases to preserve the efficiency gains of automation.

3.2. Phase 2: Relabeling and Clinical Validation

Motivated by the findings in Phase 1, we proceeded to systematically relabel the dataset to establish a more reliable ground truth. We subdivided the Phase 2 experiment process into three parts: pipeline setup, automated error definition, and independent physician validation.

Pipeline 2 Setup. We developed a separate relabeling pipeline (Fig. 4; for prompts we used, see Appendix Fig. 7) using a `Gemini-2.5-Pro` agent with access to Google Search and Python

execution capabilities. Unlike Phase 1, the agent was provided only the patient context and question (C, q), without access to the original MedCalc-Bench metadata including $\hat{y}_{\text{original}}$. We applied this pipeline to the full MedCalc test set ($n = 1{,}047$) and a stratified random sample of the training set ($n = 5{,}183$, 50% of total), stratified by question type q. To ensure label stability, each instance was processed by five independent copies this Gemini agent. If at least 4 of the 5 outputs agree in type and value (up to two decimal places for reals, exactly for datetimes, or all abstain), we keep that supermajority value as the new label $\hat{y}_{\text{new}}$; otherwise the instance is left unlabeled by Pipeline 2. This yields a set of "high-confidence" new labels.

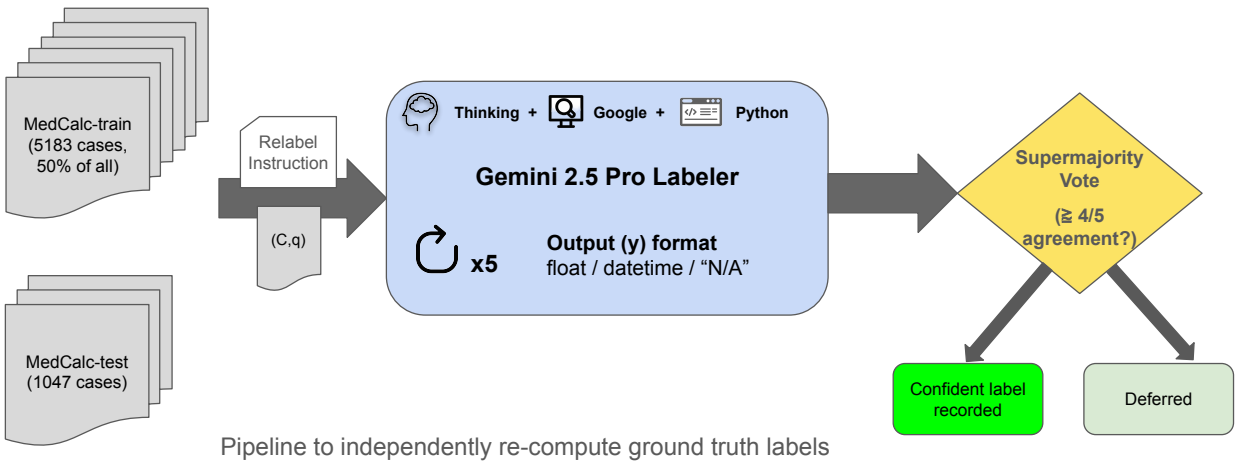

Figure 4 Phase 2 labeling pipeline. The Gemini agent sees only (C, q), has access to Google search and a code interpreter, and is asked to compute a label from first principles. For each instance we obtain five independent outputs $\hat{y}^{(1)}_{\text{new}}, \ldots, \hat{y}^{(5)}_{\text{new}}$. If at least four runs agree in type and value (up to two decimal places for reals, exact for datetimes or NA), we keep the supermajority value as the new label $\hat{y}_{\text{new}}$; otherwise, the instance is deferred.

Flagging likely label errors. Once a high-confidence $\hat{y}_{\text{new}}$ is collected from Pipeline 2 for a test instance (C, q), we compare it to $\hat{y}_{\text{original}}$. We define a symmetric discrepancy metric

$$\text{rel_err}(\hat{y}_{\text{original}}, \hat{y}_{\text{new}}) := \frac{|\hat{y}_{\text{original}} - \hat{y}_{\text{new}}|}{\max\big(|\hat{y}_{\text{original}}|, |\hat{y}_{\text{new}}|\big)}.$$

Because the denominator uses the maximum of the two estimates, rel_err is a lower bound on the true relative error that would be obtained if either $\hat{y}_{\text{original}}$ or $\hat{y}_{\text{new}}$ exactly equaled the latent clinical ground truth $y^{\star}$. We classify an instance as `Likely Error` if $\text{rel_err}(\hat{y}_{\text{original}}, \hat{y}_{\text{new}}) > 0.05$, mirroring the $\pm 5\%$ tolerance used by MedCalc-Bench for grading model outputs. Instances where either label is NA or datetime are handled respectively by exact match and > 1 day difference.

Physician validation protocol. To obtain an external clinical reference, we asked three licensed physicians (pediatrics, anesthesiology, oncology) to independently recompute a small subset of labels. The validation proceeds in three steps. First, we sort the potentially erroneous instances flagged by the above automated procedure in descending order of relative disagreement, counting NA's as the highest disagreement. Second, physicians screened the score questions q to identify those matching their clinical specialty. Third, we selected 50 instances from the sorted list, assigning cases to reviewers based on domain alignment to ensure that every instance was validated by an expert in that specific calculator type. For each (C, q) they review, a physician saw only (C, q) and were asked to compute the score manually, without seeing either $\hat{y}_{\text{original}}$ or $\hat{y}_{\text{new}}$ (a single-blind design); physicians were allowed to label an instance as NA if they considered (C, q) clinically unanswerable / a mismatch. Each of the 50 instances was labeled once by one of the three physicians, which we treat as the gold-standard answer $y^\star$. We then quantify the relative deviation of $\hat{y}_{\text{original}}$ and $\hat{y}_{\text{new}}$ against $y^\star$ by computing two metrics: (i) sMAPE on the instances a physician deemed answerable where sMAPE is short for symmetric Mean Absolute Percentage Error (Armstrong, 1985), defined as

$$\text{sMAPE}(y^*, \hat{y}) = \frac{100\%}{N} \sum_{i=1}^{N} \frac{2 \times |y_i^* - \hat{y}_i|}{|y_i^*| + |\hat{y}_i|},$$

and (ii) count of "agreement" that counts, across all 50 instances, how often each synthetic label matches $y^\star$ within a clinically reasonable threshold, defined as $\pm 5\%$ for real numbers, exact match if $y^* = \text{NA}$, or ± 1 for ordinal numbers less than 20.

3.2.1. Phase 2 Results

Coverage and abstentions. Pipeline 2 achieved high-confidence labels for 887 out of 1,047 MedCalc test instances (85%) and for 4,593 out of 5,183 sampled train instances (89%). Among these high-confidence labels, the abstention rate, cases where Pipeline 2 output NA, was 7.4% on the test set and 5.7% on the sampled train set. Consistent with our discussion in §3.1, we retain such NA instances in the relabeled benchmark, as they correspond to clinically relevant "cannot be computed" cases rather than noise.

Estimated rate of likely mislabels. Among the 887 test instances with high-confidence $\hat{y}_{\text{new}}$, we find that 220 (24.8%) exceed the $\pm 5\%$ numerical discrepancy threshold and are flagged as `Likely Error` under rel_err, plus another 66 (7.4%) are flagged as NA. Together, this implies a total of 32.2% of the original test instances as likely mislabeled. We note that this is still likely an underestimate, as rel_err is a conservative, symmetric lower bound on the underlying relative error with respect to the unknown $y^\star$. Moreover, the 160 test instances for which Pipeline 2 could *not* reach a supermajority (and are therefore excluded from this calculation) are plausibly hard cases where both $\hat{y}_{\text{original}}$ and $\hat{y}_{\text{new}}$ may be less reliable, potentially pushing the true mislabel rate above 32.2%.

Table 3 Original MedCalc test labels ($\hat{y}_{\text{original}}$) and our revised labels ($\hat{y}_{\text{new}}$) against 50 physician-generated labels ($y^\star$). sMAPE, short for symmetric Mean Absolute Percentage Error, reports the average relative percentage deviation from physicians' labels; it is computed on 34 / 33 instances where the $y^\star$ and $\hat{y}_{\text{original}}$ / $\hat{y}_{\text{new}}$ are both numeric values. "Agreement" counts how many predicted labels in a group match the physician label up to a reasonable threshold. Square brackets are bootstrap 95% confidence intervals.

Metric	$\hat{y}_{\text{original}}$	$\hat{y}_{\text{new}}$
sMAPE (%)	72.7 [47.9, 99.1]	**20.1** [8.0, 35.9]
Agreement	10/50 (20.0%)	**37/50 (74.0%)**

Physician validation. Table 3 quantifies the prediction accuracy of $\hat{y}_{\text{original}}$ and $\hat{y}_{\text{new}}$ on the set of test instances with physician-computed labels, which we have treated as $y^\star$. Across the 50 instances, $\hat{y}_{\text{new}}$ agrees with $y^\star$ 37 times, compared to $\hat{y}_{\text{original}}$'s 10 times. Beyond binary agreement, the new labels drive sMAPE down from 72.7% to 20.1%, meaning that $\hat{y}_{\text{new}}$ typically lies much closer to physicians' numerical assessments in both absolute and relative terms. Although the sample size is modest, these results provide a targeted reality check that the relabeled $\hat{y}_{\text{new}}$'s are more aligned with expert judgment on a substantial fraction of the contentious cases revealed by Pipeline 2.

3.2.2. Phase 2 Qualitative Analysis

Single-blind physician recomputations suggest that a substantial share of label disagreement is driven not by arithmetic mistakes, but by *task underspecification*: many instances do not contain enough contextual qualifiers to define a unique clinical "ground truth" score. Two patterns recur. First, the benchmark rarely specifies a scoring *timepoint*. Many notes describe multi-visit trajectories over weeks or months, but the question does not clarify whether the score should be computed at presentation, peak severity, discharge, or another reference time (e.g. rows 138, 334, 341, 509, 569, 739, 761, 785). Second, scoring rules can vary across time and jurisdiction, so the "official" aggregation rule (our g_ϕ) is not uniquely describable by a static benchmark label. For example, Morphine Milligram Equivalent (MME) conversions for methadone depend on which guideline is assumed: pre-2023 CDC guidance used a tiered rule, i.e. a multiplier of 12 for methadone doses > 60 mg/day (CDC, 2016), whereas the current CDC guideline adopts a flatter multiplier (4.7) while cautioning that conversion becomes unreliable at higher doses (Dowell et al., 2022); some state-level guidance still reflects the earlier schedule (Maryland Department of Health, 2025; Utah Department of Health and Human Services, 2025). Under either ambiguity, multiple defensible answers exist, so a single numeric gold label does not cleanly measure an LLM's generalizable clinical capability.

Beyond underspecification, physician review also surfaced outright (C, q) mismatches that induce a *distribution shift*: the patient context falls outside the population for which the calculator was derived or validated. A clear example is row 328, where the question asks for maintenance fluids for a 1.1 kg cat, despite the underlying dosing heuristic being estimated on humans. In such cases,

forcing computation produces a clinically meaningless quantity. These instances are better treated as abstentions (NA) or excluded from accuracy-based evaluation, and the benchmark prompt should explicitly allow safe non-response when (C, q) is clinically incompatible.

Practically, these failure modes motivate adding metadata (timepoint + guideline/version) and expanding the label space to include abstention.

4. When Labels Become Rewards and a Yardstick: A Controlled Study of Label Choice in Model Alignment

§3 argued that MedCalc-Bench's original labels are often misaligned with clinical reality and introduced a relabeled version with closer agreement to physicians. Because this benchmark is also used to train LLMs, *label alignment* is not only an evaluation concern: it directly shapes the behavior of next-generation models that are optimized to match these labels.

The primary goal of this section is to investigate whether the label discrepancies documented above have a meaningful impact on downstream model training, or whether such noise is effectively "washed out" by the strength of signal in the data. This is not a foregone conclusion: when training on thousands of examples, one might expect that moderate label noise would be absorbed and have little effect on final model accuracy. Conversely, if label choice does materially affect trained model performance, this would underscore the practical importance of benchmark maintenance efforts like ours.

To test this, we view model alignment as a reinforcement learning (RL) stage in which a base model is iteratively updated to maximize a reward defined with respect to benchmark labels. Changing from MedCalc's original labels $\hat{y}_{\mathsf{original}}$ to our corrected labels $\hat{y}_{\mathsf{new}}$ is therefore equivalent to changing the reward function and, by extension, the model's implicit alignment objective. We run a controlled comparison study in which the same RL training pipeline is applied to Qwen3-8B with only the reward labels varied, holding all other factors constant. Crucially, in our experimental design, both the training rewards and the evaluation metric are defined with respect to the corrected labels $\hat{y}_{\mathsf{new}}$. This means the comparison is not strictly apples-to-apples if one believes the two label sets differ meaningfully. However, this is precisely the point: if $\hat{y}_{\mathsf{original}}$ and $\hat{y}_{\mathsf{new}}$ were interchangeable up to inconsequential noise, we would expect both training conditions to yield similar test accuracy. A substantial performance gap would rule out this null hypothesis and demonstrate that the label discrepancies have real downstream consequences.

We emphasize that our goal is *not* to claim state-of-the-art benchmark performance. Rather, we seek to establish that label quality has tangible consequences for model alignment. That said, if one accepts the evidence from §3 that the corrected labels more closely reflect clinical ground truth, then a model trained on these labels would, in principle, be better aligned with physician judgment.

We consider this a secondary implication and leave more rigorous validation of this claim—including broader physician evaluation of model outputs—to future work. The primary contribution of this section is simply to demonstrate that the choice of benchmark labels is not merely a measurement detail, but a consequential design decision that shapes the models we build.

4.1. Model alignment as policy optimization

We adopt a standard sequential decision-making formalism for model alignment, following the RL literature on policy-gradient methods and recent work on LLM post-training.[3] In this view, the interaction between an LLM agent and its digital environment is a Markov decision process (MDP) $(\mathcal{S}, \mathcal{A}, R, P, \mu)$: at each discrete time $t = 1, \ldots, T$ the agent observes a state $s_t \in \mathcal{S}$, samples an action $a_t \in \mathcal{A}$ from a stochastic policy $\pi_\theta(a_t \mid s_t)$, receives a reward $r_t = R(s_t, a_t, s_{t+1})$, and the environment transitions to $s_{t+1} \sim P(\cdot \mid s_t, a_t)$. A trajectory (i.e. a token sequence for an LLM) is

$$\tau = (s_1, a_1, s_2, a_2, \ldots, s_T, a_T, s_{T+1}),$$

with initial state $s_1 \sim \mu$. The policy objective is to maximize the expected return

$$J(\theta) = \mathbb{E}_{\tau \sim p_\theta(\tau)}[R(\tau)] = \int p_\theta(\tau) R(\tau)\, d\tau, \quad R(\tau) = \sum_{t=1}^{T} r_t, \tag{1}$$

where $p_\theta(\tau)$ is the trajectory distribution induced by π_θ and the MDP dynamics.

Instantiating the MDP for MedCalc-Bench. For an LLM, the state s_t is the current token sequence cached in the GPU memory (prompt, EHR snippet, and previously generated tokens), the action a_t is the next token, and the transition is deterministic: $s_{t+1} = (s_t, a_t)$. The initial state $s_1 \sim \mu$ corresponds to a prompt i.e. (C, q) randomly sampled from the set of MedCalc-Bench instances. In classical MDP formulations, returns are often written as a sum of stepwise rewards like the second equation in (1). However, in LLM post-training a simpler, *outcome-based* interpretation is more often assumed. Given an input $(C, q) := x$ and a final answer $y(\tau)$ parsed from a completed text trajectory τ, we set $r_t = 0$ for all $t < T$ such that the trajectory-level reward becomes

$$R(\tau) = r_T := \underbrace{\lambda_{\text{f}} \cdot \mathbf{1}\{\, \hat{y}(\tau) \text{ is parsable} \,\}}_{\text{format reward}} + (1 - \lambda_{\text{f}}) \cdot \underbrace{\mathbf{1}\{\, \text{rel_err}(\hat{y}(\tau), y^*) \leq \epsilon \,\}}_{\text{answer reward}} \tag{2}$$

that combines correctness of the computed score and adherence to the required output format for regex parsability, evaluated against a gold label y^* (surrogated by either $\hat{y}_{\text{original}}$ or $\hat{y}_{\text{new}}$). In this abstraction, varying y^*'s value corresponds exactly to changing the reward function R in the MDP.

[3] See, e.g. Williams (1992); Sutton et al. (1999); Schulman et al. (2016); Kool et al. (2019); Ouyang et al. (2022); Ahmadian et al. (2024); Guo et al. (2025); Kumar et al. (2025).

Policy gradient and REINFORCE. To optimize (1), we differentiate under the integral and apply the log-derivative identity $\nabla_\theta p_\theta(x) = p_\theta(x)\nabla_\theta \log p_\theta(x)$:

$$\nabla_\theta J(\theta) \;=\; \int \nabla_\theta p_\theta(\tau)\, R(\tau)\, d\tau \;=\; \mathbb{E}_{\tau\sim p_\theta(\tau)}[R(\tau)\,\nabla_\theta \log p_\theta(\tau)]\,.$$

Because $p_\theta(\tau)$ factors as

$$p_\theta(\tau) = \mu(s_1)\prod_{t=1}^{T}\pi_\theta(a_t \mid s_t)\, P(s_{t+1} \mid s_t, a_t),$$

we obtain the vanilla REINFORCE policy gradient

$$\nabla_\theta J(\theta) = \mathbb{E}_{\tau\sim p_\theta(\tau)}\left[R(\tau)\sum_{t=1}^{T}\nabla_\theta \log \pi_\theta(a_t \mid s_t)\right]. \tag{3}$$

A standard variance-reduction trick is to subtract a zero-mean baseline b that does not depend on the realized value of τ:

$$\nabla_\theta J(\theta) = \mathbb{E}_{\tau\sim p_\theta(\tau)}\left[\big(R(\tau) - b\big)\sum_{t=1}^{T}\nabla_\theta \log \pi_\theta(a_t \mid s_t)\right]. \tag{4}$$

This is the *REINFORCE with baseline* estimator in the trajectory-level reward setting we use: every token on a trajectory shares the same scalar credit signal $R(\tau) - b$.

Group-relative policy optimization (GRPO). GRPO specializes (4) by using a *group-relative* baseline at the level of each initial state s_1 (think a (C, q) tuple in MedCalc-Bench). Fix a group size G (e.g. 8), then for every s_1 we sample G trajectories $\{\tau^{(i)}\}_{i=1}^{G}$ under the current policy π_θ, compute their trajectory-level rewards $R^{(i)} = R(\tau^{(i)})$, form the group average $\bar{R}$ and define advantages $A^{(i)}$

$$\bar{R} \;=\; \frac{1}{G}\sum_{i=1}^{G} R^{(i)}, \quad A^{(i)} \;=\; R^{(i)} - \bar{R}, \tag{5}$$

so that trajectory samples with above-average reward receive positive credit and those with below-average reward receive negative credit, finally back-propagated into LLM weight updates.

In our simplified on-policy implementation, the GRPO loss for updating θ is

$$L_{\mathrm{GRPO}}(\theta) = -\,\mathbb{E}_{\{\tau^{(i)}\}_{i=1}^{G}\sim p_\theta(\cdot|s_1)}\left[\sum_{i=1}^{G} A^{(i)}\sum_{t=1}^{T^{(i)}}\log \pi_\theta\big(a_t^{(i)} \mid s_t^{(i)}\big)\right] \;+\; \beta\cdot \mathrm{KL}(\pi_\theta \,\|\, \pi_{\mathrm{ref}})\,, \tag{6}$$

where $T^{(i)}$ is the length of trajectory $\tau^{(i)}$, π_{ref} is a fixed reference policy, and $\beta > 0$ controls the strength of KL regularization. Minimizing (6) corresponds to a REINFORCE-style policy update that (i) increases the log-probability of completions whose reward is higher than their group mean and (ii) keeps the updated policy close to π_{ref} to avoid catastrophic forgetting.

In summary, under this MDP and GRPO formalism, instantiating the benchmark labels y^* by $\hat{y}_{\mathrm{original}}$ or $\hat{y}_{\mathrm{new}}$ shapes the reward assignment $R(\tau)$ in (2), and therefore the advantages $A^{(i)}$ in (5). The rest of the policy-optimization pipeline is held fixed, so any difference in the fine-tuned π_θ's test accuracy can be attributed to the choice of labels used to define the alignment objective.

4.2. Controlled Study Setup

Goal and overall design. Our goal is to isolate the causal effect of label choice on an LLM's model alignment when RL is used. To this end, we run two GRPO training experiments on the same base model that are identical in all respects except for the labels used to define the training reward. In the *original-label* arm, training rewards (as assigned by (2)) are computed against MedCalc-Bench's original labels $\hat{y}_{\text{original}}$; in the *new-label* arm, training rewards are computed against our corrected labels $\hat{y}_{\text{new}}$. At test time, the 0-1 accuracy of both models are always graded against $\hat{y}_{\text{new}}$, which our Phase 2 study (§3.2.1) found to be more clinically accurate than $\hat{y}_{\text{original}}$.

Dataset and label conditions. Both RL runs are trained on the same subset of 4,593 MedCalc-Bench train instances for which Pipeline 2 produced high-confidence $\hat{y}_{\text{new}}$ labels. The held-out test set consists of 887 instances whose $\hat{y}_{\text{new}}$ labels were also obtained from Pipeline 2 and partially audited by physicians. In both arms, the policy LLM sees exactly the same collection of prompts and calculator types; the only difference is whether the training reward's y^* is instantiated using $\hat{y}_{\text{original}}$ or $\hat{y}_{\text{new}}$. The underlying system and user prompts, including chain-of-thought and answer-format instructions, are held fixed across runs; we provide the full prompt template in the Appendix.

Policy initialization and interaction environment. In both arms, the trainable policy π_θ and the frozen reference policy π_{ref} are initialized from the same Qwen3-8B base model (Qwen, 2025), chosen as a widely used open model for academic post-training. π_{ref}, being used for KL regularization, remains fixed throughout training, while π_θ is updated iteratively by gradient descent to minimize the GRPO loss in Eq. 6. We use the same updated system prompt (which allows for abstention) and require chain-of-thought style completions with a final scalar answer token; no external tools are used during RL training, and the interaction is purely text-based.

Key training hyperparameters. We instantiate the policy objective from §4.1 using the trajectory-level reward $r(\tau)$ in Eq. 2 with $\lambda_f = 0.1$. For the comparison experiment in §4.3, both runs share the same optimizer and hyperparameters: Adam with learning rate $\text{lr} = 10^{-5}$, KL regularization coefficient $\beta = 10^{-3}$, and no reward standardization or length normalization to ensure advantage estimation is unbiased (Liu et al., 2025b). Each GRPO minibatch consists of 256 distinct (C, q) pairs from the MedCalc training set. We maintain the same random seed so that the minibatch partitions and ordering are identical between the two runs. We also conducted a hyperparameter sensitivity analysis over the learning rates $\{10^{-4}, 10^{-5}, 10^{-6}\}$ and KL coefficient $\{10^{-2}, 10^{-3}, 10^{-4}\}$.

Sampling and evaluation protocol. During training, all trajectories are generated from π_θ with a temperature of 1.0, top-$p = 1.0$, and a maximum output length of 1600 tokens. Moreover, the GRPO group size $G = 8$, i.e. 8 trajectories are sampled i.i.d. from π_θ for each (C, q) pair in a minibatch. After training, we evaluate the two policies on the 887-instance held-out test set, with ths same inference configuraiton as training rollouts. The evaluation metric is the 0-1 test accuracy defined

in §3.2: we parse the model's final scalar score (or abstention token) and compare it against the physician-audited $\hat{y}_{\text{new}}$ labels, treating abstentions as correct only when $\hat{y}_{\text{new}}$ is NA. All decision rules—prompts, reward shape, decoding, and accuracy metric—are held fixed across the two training runs; only the training labels used inside $r(\tau)$ differ.

Hardware and implementation summary. Both training runs are conducted on an 8×H100 GPU node with two 56-core Intel 8480C CPUs for 9 hours, using the `verl` (Sheng et al., 2024) framework for distributed RL training. The experiment run in Fig. 5 consumes $2 \times (8 \times 9) = 144$ GPU hours; if including the sensitivity analysis, our experiment consumes $144 \times (3 \times 3) = 1296$ GPU hours.

4.3. Comparison Results

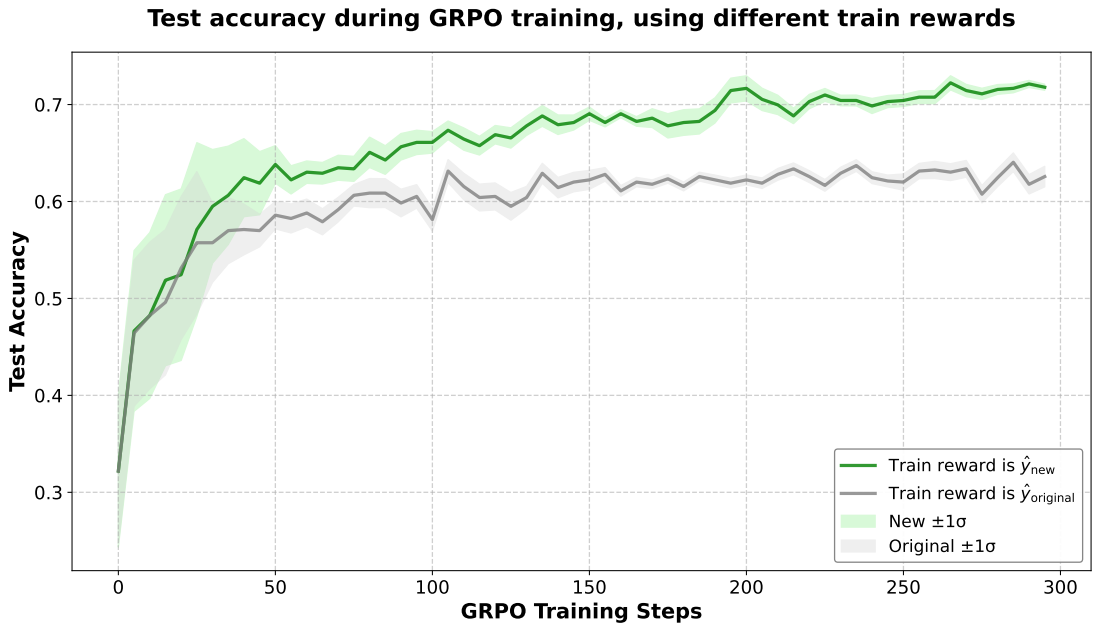

Figure 5 Impact of Label Alignment on Model Alignment. Test accuracy dynamics for Qwen3-8B trained via GRPO using our clinically corrected labels (green) versus the original benchmark labels (grey). Shaded bands indicate $\pm 1\sigma$ smoothed over a 10-step window. Improving the reward signal's factual grounding yields a $+8.7\%$ absolute gain in the final moving averages of model test accuracy (71.4% vs. 62.6%).

We present the dynamics of test accuracy during training in Figure 5. Both policies converge after approximately 200 GRPO steps. Averaging the final ten evaluation steps, the policy trained on our corrected labels ($\hat{y}_{\text{new}}$) achieves a final accuracy of 71.4%, whereas the policy trained on the original benchmark labels ($\hat{y}_{\text{original}}$) plateaus at 62.6%. This constitutes a substantial +8.7% absolute improvement attributable solely to the quality of the reward signal.

To contextualize this result, we note that a 8.7% performance gap is large relative to recent advances in this domain; for instance, it is comparable to the gains often reported between different

alignment algorithms (see Table 2). It is also worth noting that while the label discrepancy between $\hat{y}_{\text{original}}$ and $\hat{y}_{\text{new}}$ is roughly 32% (see §3.2.1), the downstream performance degradation is smaller (8.7%), suggesting that the RL process displays some resilience to noisy rewards, yet still benefits significantly from cleaner supervision.

Crucially, these results were obtained using standard, default hyperparameters for Qwen3-8B ($\text{lr} = 10^{-5}$, $\beta = 10^{-3}$, $\lambda_f = 0.1$), selected *a priori* without searching for a configuration that favors our method. In addition, the sensitivity analysis we performed over a 3×3 hyperparameter sweep confirms that this performance difference is salient across all nine configurations.

5. Discussion

In this work, we showed that a widely used, mostly LLM-labeled clinical computation benchmark has between one-quarter and one-third of test instances that appear mislabeled, affecting both measured performance and downstream model alignment. Our formal analysis and empirical audits explain how the original data-generating process for MedCalc-Bench's ground truth causes systematic output errors. The physician-in-the-loop system, instantiated via two automated pipelines, identifies substantially more likely label errors per unit of physician time than uniform sampling, and yields revised labels that physicians judge as more clinically aligned.

Our controlled RL experiment was designed not to claim superior benchmark performance, but to test whether label discrepancies have meaningful downstream consequences or are simply absorbed as noise during training. The substantial accuracy gap we observe (8.7%) rules out the latter hypothesis, demonstrating that benchmark label quality is not merely a measurement detail but a consequential factor in model alignment. If one accepts the evidence from §3 that the corrected labels better reflect clinical ground truth, then it follows that models trained on these labels would be better aligned with physician judgment—but we consider this a secondary implication and leave rigorous validation to future work.

Together, these findings suggest that clinical benchmarks built with partial LLM inputs should be treated as *living documents*, whose labels co-evolve with both physician feedback and model capabilities. In safety-critical domains, such ongoing maintenance is not optional: benchmarks must be revisited as clinical practice and model capabilities change.

5.1. Limitations

Our study has several limitations. First, the human expert reference used to validate label alignment is high quality but small. Only three physicians from a single healthcare system participated in the blinded review, and they independently computed labels for 50 contentious test instances. While these labels provide a valuable sanity check that our relabeled $\hat{y}_{\text{new}}$'s are much closer to expert

judgment than the original $\hat{y}_{\text{original}}$'s, a larger panel of physician experts, with the same instances receiving multiple independent labels, would be needed to robustly quantify systematic variability.

Second, our automated pipelines depend on a particular family of LLM verifiers (Gemini-2.5-Pro with search and tools) instantiated with a fixed prompting and tool-use strategy. If Gemini's failure modes are correlated with those of GPT-4 (used in the original MedCalc-Bench labels) or with the downstream models we wish to evaluate, some systematic error patterns may never be surfaced. Our estimates of the mislabel rate are therefore conditional on this specific verifier.

Third, our automated label verification has incomplete coverage. Pipeline 2 produces high-confidence labels for 85% of MedCalc's test set and 89% of the sampled train set; the remaining instances where the pipeline fails to reach a supermajority are plausibly the hardest cases, and may be precisely those where physician input matters most. We exclude these deferred instances from our main analyses, meaning that both the estimated mislabel rate and the measured effect of label choice on RL alignment are computed on a more auditor-tractable subset.

Finally, our experiments focus on a narrow but important slice of clinical AI: MDCalc-style risk and severity scores derived from English-language case reports. Real-world EHRs are substantially noisier, often interleaving templated text, missing or conflicting entries, and non-English content. We also instantiate our RL study with a single base model (Qwen3-8B) and one algorithm (GRPO). Although our sensitivity analysis suggests the relative benefit of aligned labels is robust across hyperparameter settings, we do not claim that the magnitude of the effect will transfer unchanged to other architectures or task families.

5.2. Future Work

A central lesson from our study is that the real bottleneck in benchmark maintenance is not computation, but carefully allocated human attention. GPU hours are elastic; physicians' hours are not. This naturally leads to a design question: given a fixed budget of expert feedback, how should we allocate human evaluation to learn as much as possible about benchmark quality?

Conceptually, there is a latent error structure describing where labels are wrong and which calculators are fragile, and each physician review is a costly observation about that structure. Future work could formalize benchmark maintenance as choosing queries that maximize expected information gain about this latent structure per unit of expert time. Our two-pipeline system can be viewed as a heuristic approximation: LLM auditors concentrate mass on contentious cases, and physicians act as high-leverage adjudicators rather than bulk labelers. The same information-efficient perspective applies upstream to benchmark *creation*—recent work such as GDPval (Patwardhan et al., 2025) illustrates how task selection and expert effort allocation shape benchmark design in several domains. Coupling explicit uncertainty models over labels with active-learning or bandit-style policies for expert review is a promising direction we leave to future work.

Acknowledgments

Some of the computing for this project was performed on the Stanford Marlowe GPU cluster (Kapfer et al., 2025). We thank Stanford University and Stanford Data Science for providing the computational resources at a subsidized rate that made these research results possible.

References

Acimovic, Jason, Stephen C. Graves. 2015. Making better fulfillment decisions on the fly in an online retail environment. *Manufacturing & Service Operations Management* **17**(1) 34–51. doi:10.1287/msom.2014.0505.

Ahmadian, Arash, Chris Cremer, Matthias Gallé, Marzieh Fadaee, Julia Kreutzer, Olivier Pietquin, Ahmet Üstün, Sara Hooker. 2024. Back to basics: Revisiting reinforce-style optimization for learning from human feedback in llms. *Proceedings of the 62nd Annual Meeting of the Association for Computational Linguistics (Volume 1: Long Papers)*. 12248–12267.

Armstrong, J. Scott. 1985. *Long-Range Forecasting: From Crystal Ball to Computer*. 2nd ed. John Wiley & Sons, New York. URL `https://ssrn.com/abstract=666990`.

Aswani, Anil, Zuo-Jun Max Shen, Auyon Siddiq. 2019. Data-driven incentive design in the Medicare shared savings program. *Operations Research* **67**(4) 1002–1026. doi:10.1287/opre.2018.1821.

Athey, Susan, Stefan Wager. 2021. Policy learning with observational data. *Econometrica* **89**(1) 133–161. doi:10.3982/ECTA15732.

Ban, Gah-Yi, Cynthia Rudin. 2019. The Big Data newsvendor: Practical insights from machine learning. *Operations Research* **67**(1) 90–108. doi:10.1287/opre.2018.1757.

Bastani, Hamsa, Mohsen Bayati. 2020. Online decision making with high-dimensional covariates. *Operations Research* **68**(1) 276–294. doi:10.1287/opre.2019.1902.

Bayati, Mohsen, Mark Braverman, Michael Gillam, Karen M. Mack, George Ruiz, Mark S. Smith, Eric Horvitz. 2014. Data-driven decisions for reducing readmissions for heart failure: General methodology and case study. *PLOS ONE* **9**(10) e109264. doi:10.1371/journal.pone.0109264.

Bedi, Suhana, Hejie Cui, Miguel Fuentes, Alyssa Unell, Michael Wornow, Juan M Banda, Nikesh Kotecha, Timothy Keyes, Yifan Mai, Mert Oez, et al. 2025. MedHELM: Holistic evaluation of large language models for medical tasks. *arXiv preprint arXiv:2505.23802* .

Bertsimas, Dimitris, Nathan Kallus. 2020. From predictive to prescriptive analytics. *Management Science* **66**(3) 1025–1044. doi:10.1287/mnsc.2018.3253.

Bertsimas, Dimitris, Adam J. Mersereau. 2007. A learning approach for interactive marketing to a customer segment. *Operations Research* **55**(6) 1120–1135. doi:10.1287/opre.1070.0427.

Bertsimas, Dimitris, Aurélie Thiele. 2006. A robust optimization approach to inventory theory. *Operations Research* **54**(1) 150–168. doi:10.1287/opre.1050.0238.

Besbes, Omar, Assaf Zeevi. 2009. Dynamic pricing without knowing the demand function: Risk bounds and near-optimal algorithms. *Operations Research* **57**(6) 1407–1420. doi:10.1287/opre.1080.0640.

CDC. 2016. Calculating Total Daily Dose of Opioids for Safer Dosage. U.S. Department of Health and Human Services. URL `https://web.archive.org/web/20221125005318/https:`

//www.cdc.gov/drugoverdose/pdf/calculating_total_daily_dose-a.pdf. Archived from the original on November 25, 2022.

Chick, Stephen E., Noah Gans. 2009. Economic analysis of simulation selection problems. *Management Science* **55**(3) 421–437. doi:10.1287/mnsc.1080.0949.

Comanici, Gheorghe, Eric Bieber, Mike Schaekermann, Ice Pasupat, Noveen Sachdeva, Inderjit Dhillon, Marcel Blistein, Ori Ram, Dan Zhang, Evan Rosen, et al. 2025. Gemini 2.5: Pushing the frontier with advanced reasoning, multimodality, long context, and next generation agentic capabilities. *arXiv preprint arXiv:2507.06261* .

Delage, Erick, Yinyu Ye. 2010. Distributionally robust optimization under moment uncertainty with application to data-driven problems. *Operations Research* **58**(3) 595–612. doi:10.1287/opre.1090.0741.

den Boer, Arnoud V., Bert Zwart. 2014. Simultaneously learning and optimizing using controlled variance pricing. *Management Science* **60**(3) 770–783. doi:10.1287/mnsc.2013.1788.

Dowell, Deborah, Kathleen R. Ragan, Christopher M. Jones, Grant T. Baldwin, Roger Chou. 2022. CDC clinical practice guideline for prescribing opioids for pain — United States, 2022. *MMWR Recommendations and Reports* **71**(3) 1–95. doi:10.15585/mmwr.rr7103a1. URL https://www.cdc.gov/mmwr/volumes/71/rr/rr7103a1.htm.

Elmachtoub, Adam N., Paul Grigas. 2022. Smart "predict, then optimize". *Management Science* **68**(1) 9–26. doi:10.1287/mnsc.2020.3922.

Ferreira, Kris Johnson, Bin Hong Alex Lee, David Simchi-Levi. 2016. Analytics for an online retailer: Demand forecasting and price optimization. *Manufacturing & Service Operations Management* **18**(1) 69–88. doi:10.1287/msom.2015.0561.

Goodell, Alex J, Simon N Chu, Dara Rouholiman, Larry F Chu. 2025. Large language model agents can use tools to perform clinical calculations. *npj Digital Medicine* **8**(1) 163.

Guo, Daya, Dejian Yang, Haowei Zhang, Junxiao Song, Ruoyu Zhang, Runxin Xu, Qihao Zhu, Shirong Ma, Peiyi Wang, Xiao Bi, et al. 2025. Deepseek-r1: Incentivizing reasoning capability in llms via reinforcement learning. *arXiv preprint arXiv:2501.12948* .

Han, Shasha, Tait D Shanafelt, Christine A Sinsky, Karim M Awad, Liselotte N Dyrbye, Lynne C Fiscus, Mickey Trockel, Joel Goh. 2019. Estimating the attributable cost of physician burnout in the united states. *Annals of internal medicine* **170**(11) 784–790.

Harrison, J. Michael, N. Bora Keskin, Assaf Zeevi. 2012. Bayesian dynamic pricing policies: Learning and earning under a binary prior distribution. *Management Science* **58**(3) 570–586. doi:10.1287/mnsc.1110.1426.

Jin, Qiao, Zhizheng Wang, Yifan Yang, Qingqing Zhu, Donald Wright, Thomas Huang, Nikhil Khandekar, Nicholas Wan, Xuguang Ai, W John Wilbur, et al. 2025. Agentmd: Empowering

language agents for risk prediction with large-scale clinical tool learning. *Nature Communications* **16**(1) 9377.

Kapfer, Craig, Kurt Stine, Balasubramanian Narasimhan, Christopher Mentzel, Emmanuel Candes. 2025. Marlowe: Stanford's gpu-based computational instrument. `https://doi.org/10.5281/zenodo.14751899`. doi:10.5281/zenodo.14751899. Stanford Data Science report.

Katehakis, Michael N., Jr. Veinott, Arthur F. 1987. The multi-armed bandit problem: Decomposition and computation. *Mathematics of Operations Research* **12**(2) 262–268. doi:10.1287/moor.12.2.262.

Khandekar, Nikhil, Qiao Jin, Guangzhi Xiong, Soren Dunn, Serina Applebaum, Zain Anwar, Maame Sarfo-Gyamfi, Conrad Safranek, Abid Anwar, Andrew Zhang, et al. 2024. Medcalc-bench: Evaluating large language models for medical calculations. *Advances in Neural Information Processing Systems* **37** 84730–84745.

Kitagawa, Toru, Aleksey Tetenov. 2018. Who should be treated? empirical welfare maximization methods for treatment choice. *Econometrica* **86**(2) 591–616. doi:10.3982/ECTA13288.

Kool, Wouter, Herke van Hoof, Max Welling. 2019. Buy 4 REINFORCE samples, get a baseline for free! URL `https://openreview.net/forum?id=r1lgTGL5DE`. ICLR 2019 Workshop drlStructPred.

Korom, Robert, Sarah Kiptinness, Najib Adan, Kassim Said, Catherine Ithuli, Oliver Rotich, Boniface Kimani, Irene King'ori, Stellah Kamau, Elizabeth Atemba, Muna Aden, Preston Bowman, Michael Sharman, Rebecca Soskin Hicks, Rebecca Distler, Johannes Heidecke, Rahul K. Arora, Karan Singhal. 2025. AI-based clinical decision support for primary care: A real-world study. *arXiv preprint arXiv:2507.16947* URL `https://arxiv.org/abs/2507.16947`.

Kumar, Aviral, Vincent Zhuang, Rishabh Agarwal, Yi Su, John D Co-Reyes, Avi Singh, Kate Baumli, Shariq Iqbal, Colton Bishop, Rebecca Roelofs, et al. 2025. Training language models to self-correct via reinforcement learning. *The Thirteenth International Conference on Learning Representations*.

Lim, W.S., M.M. van der Eerden, R. Laing, W.G. Boersma, N. Karalus, G.I. Town, S.A. Lewis, J.T. Macfarlane. 2003. Defining community acquired pneumonia severity on presentation to hospital: an international derivation and validation study. *Thorax* **58**(5) 377–382.

Lin, Jiacheng, Zhenbang Wu, Jimeng Sun. 2025. Training llms for ehr-based reasoning tasks via reinforcement learning. URL `https://arxiv.org/abs/2505.24105`.

Lip, Gregory Y.H., Robby Nieuwlaat, Ron Pisters, Deirdre A. Lane, Harry J.G.M. Crijns. 2010. Refining clinical risk stratification for predicting stroke and thromboembolism in atrial fibrillation using a novel risk factor-based approach: the euro heart survey on atrial fibrillation. *Chest* **137**(2) 263–272.

Liu, Fenglin, Jinge Wu, Hongjian Zhou, Xiao Gu, Soheila Molaei, Anshul Thakur, Lei A. Clifton, Honghan Wu, David A. Clifton. 2025a. Riskagent: Autonomous medical ai copilot for generalist risk prediction. *CoRR* **abs/2503.03802**. URL `https://doi.org/10.48550/arXiv.2503.03802`.

Liu, Zichen, Changyu Chen, Wenjun Li, Penghui Qi, Tianyu Pang, Chao Du, Wee Sun Lee, Min Lin. 2025b. Understanding r1-zero-like training: A critical perspective. *arXiv preprint arXiv:2503.20783* .

Liyanage, Liwan H., J. George Shanthikumar. 2005. A practical inventory control policy using operational statistics. *Operations Research Letters* **33**(4) 341–348. doi:10.1016/j.orl.2004.08.003.

Manski, Charles F. 2004. Statistical treatment rules for heterogeneous populations. *Econometrica* **72**(4) 1221–1246. doi:10.1111/j.1468-0262.2004.00530.x.

Maryland Department of Health. 2025. PDMP Morphine Milligram Equivalents Fact Sheet. URL `https://web.archive.org/web/20250831211406/https://health.maryland.gov/pdmp/Documents/Clinical%20Docs/MME%20Fact%20Sheet.pdf`. Prescription Drug Monitoring Program. Archived from the original on August 31, 2025.

MDCalc. 2024. Frequently asked questions. `https://web.archive.org/web/20240405155011/https://www.mdcalc.com/faq`.

Muir, K. Jane, Tanya N. Wanchek, Jennifer M. Lobo, Jessica Keim-Malpass. 2022. Evaluating the costs of nurse burnout-attributed turnover: A markov modeling approach. *Journal of Patient Safety* **18**(4) 351–357. doi:10.1097/PTS.0000000000000920.

Oh, Gyutaek, Seoyeon Kim, Sangjoon Park, Byung-Hoon Kim. 2025. Rethinking test-time scaling for medical ai: Model and task-aware strategies for llms and vlms. *arXiv preprint arXiv:2506.13102* .

Ouyang, Long, Jeffrey Wu, Xu Jiang, Diogo Almeida, Carroll Wainwright, Pamela Mishkin, Chong Zhang, Sandhini Agarwal, Katarina Slama, Alex Ray, et al. 2022. Training language models to follow instructions with human feedback. *Advances in neural information processing systems* **35** 27730–27744.

Pais, Cristobal, Jianfeng Liu, Robert Voigt, Vin Gupta, Elizabeth Wade, Mohsen Bayati. 2024. Large language models for preventing medication direction errors in online pharmacies. *Nature medicine* **30**(6) 1574–1582.

Patwardhan, Tejal, Rachel Dias, Elizabeth Proehl, Grace Kim, Michele Wang, Olivia Watkins, Simón Posada Fishman, Marwan Aljubeh, Phoebe Thacker, Laurance Fauconnet, et al. 2025. Gdpval: Evaluating ai model performance on real-world economically valuable tasks. *arXiv preprint arXiv:2510.04374* .

Qwen. 2025. Qwen3 technical report. URL `https://arxiv.org/abs/2505.09388`.

Roeschl, Tobias, Marie Hoffmann, Axel Unbehaun, Henryk Dreger, Gerhard Hindricks, Volkmar Falk, Ran Balicer, Radu Tanacli, Felix Hohendanner, Alexander Meyer. 2025. Development of an llm pipeline surpassing physicians in cardiovascular risk score calculation. *medRxiv* 2025–11.

Schulman, John, Philipp Moritz, Sergey Levine, Michael Jordan, Pieter Abbeel. 2016. High-dimensional continuous control using generalized advantage estimation. *International Conference on Learning Representations (ICLR)*. URL `https://arxiv.org/abs/1506.02438`.

Shao, Zhihong, Peiyi Wang, Qihao Zhu, Runxin Xu, Junxiao Song, Xiao Bi, Haowei Zhang, Mingchuan Zhang, YK Li, Yang Wu, et al. 2024. Deepseekmath: Pushing the limits of mathematical reasoning in open language models. *arXiv preprint arXiv:2402.03300* .

Sheng, Guangming, Chi Zhang, Zilingfeng Ye, Xibin Wu, Wang Zhang, Ru Zhang, Yanghua Peng, Haibin Lin, Chuan Wu. 2024. Hybridflow: A flexible and efficient rlhf framework. *arXiv preprint arXiv: 2409.19256* .

Sinsky, Christine A., Mark Linzer, Stacy Poplau, Richard Brown, Elizabeth Williams, et al. 2022. Health care expenditures attributable to primary care physician overall and burnout-related turnover: A cross-sectional analysis. *Mayo Clinic Proceedings* **97**(4) 693–702. doi: 10.1016/j.mayocp.2021.09.013.

Song, Yuda, Hanlin Zhang, Carson Eisenach, Sham M. Kakade, Dean Foster, Udaya Ghai. 2025. Mind the gap: Examining the self-improvement capabilities of large language models. *The Thirteenth International Conference on Learning Representations*. URL `https://openreview.net/forum?id=mtJSMcF3ek`.

Sutton, Richard S, David McAllester, Satinder Singh, Yishay Mansour. 1999. Policy gradient methods for reinforcement learning with function approximation. *Advances in neural information processing systems* **12**.

Tawfik, Daniel, Mohsen Bayati, Jessica Liu, Liem Nguyen, Amrita Sinha, Thomas Kannampallil, Tait Shanafelt, Jochen Profit. 2024. Predicting primary care physician burnout from electronic health record use measures. *Mayo Clinic Proceedings* **99**(9) 1411–1421. doi:10.1016/j.mayocp.2024.01.005.

Tawfik, Daniel, Stefanie S Sebok-Syer, Cassandra Bragdon, Cati Brown-Johnson, Marcy Winget, Mohsen Bayati, Tait Shanafelt, Jochen Profit. 2025. Qualitative verification of machine learning-based burnout predictors in primary care physicians: An exploratory study. *Applied Clinical Informatics* **16**(04) 1031–1040.

Tierney, Aaron A., Gregg Gayre, Brian Hoberman, Brian Mattern, Mark Ballesca, Patrick Kipnis, Vincent Liu, Keisa Lee. 2024. Ambient artificial intelligence scribes to alleviate the burden of clinical documentation. *NEJM Catalyst Innovations in Care Delivery* **5**(3) 0404. doi:10.1056/CAT.23.0404.

Tierney, Aaron A., Gregg Gayre, Brian Hoberman, Brian Mattern, Mark Ballesca, Sarah B. Wilson Hannay, Katherine Castilla, Connie S. Lau, Patrick Kipnis, Vincent Liu, Keisa Lee. 2025. Ambient artificial intelligence scribes: Learnings after 1 year and over 2.5 million uses. *NEJM Catalyst Innovations in Care Delivery* **6**(5) 250040. doi:10.1056/CAT.25.0040.

Utah Department of Health and Human Services. 2025. Opioid Oral Morphine Milligram Equivalent (MME) Conversion Factors. URL https://web.archive.org/web/20250801184557/https://medicaid-documents.dhhs.utah.gov/Documents/files/Opioid-Morphine-EQ-Conversion-Factors.pdf. Utah Medicaid. Archived from the original on August 1, 2025.

Wang, Benlu, Iris Xia, Yifan Zhang, Junda Wang, Feiyun Ouyang, Shuo Han, Arman Cohan, Hong Yu, Zonghai Yao. 2025a. From scores to steps: Diagnosing and improving LLM performance in evidence-based medical calculations. *Proceedings of the 2025 Conference on Empirical Methods in Natural Language Processing*. Association for Computational Linguistics, Suzhou, China, 10820–10844. URL https://aclanthology.org/2025.emnlp-main.548/.

Wang, Jiayi, Jacqueline Jil Vallon, Neil Panjwani, Xi Ling, Sushmita Vij, Sandy Srinivas, John Leppert, Mark K Buyyounouski, Mohsen Bayati. 2025b. Agent-based feature generation from clinical notes for outcome prediction. *arXiv preprint arXiv:2508.01956* .

Williams, Ronald J. 1992. Simple statistical gradient-following algorithms for connectionist reinforcement learning. *Machine learning* **8**(3) 229–256.

Xie, Yunfei, Juncheng Wu, Haoqin Tu, Siwei Yang, Bingchen Zhao, Yongshuo Zong, Qiao Jin, Cihang Xie, Yuyin Zhou. 2024a. A preliminary study of o1 in medicine: Are we closer to an ai doctor? *arXiv preprint arXiv:2409.15277* .

Xie, Yunfei, Juncheng Wu, Haoqin Tu, Siwei Yang, Bingchen Zhao, Yongshuo Zong, Qiao Jin, Cihang Xie, Yuyin Zhou. 2024b. A preliminary study of o1 in medicine: Are we closer to an ai doctor? *arXiv preprint arXiv:2409.15277* .

Xu, Xiaoran, Ravi Sankar. 2025. Large language model agents for biomedicine: A comprehensive review of methods, evaluations, challenges, and future directions. *Information* **16**(10) 894.

Zhang, Xiaotian, Yuan Wang, Zhaopeng Feng, Ruizhe Chen, Zhijie Zhou, Yan Zhang, Hongxia Xu, Jian Wu, Zuozhu Liu. 2025. Med-u1: Incentivizing unified medical reasoning in llms via large-scale reinforcement learning. URL https://arxiv.org/abs/2506.12307.

Zhao, Yingqi, Donglin Zeng, A. John Rush, Michael R. Kosorok. 2012. Estimating individualized treatment rules using outcome weighted learning. *Journal of the American Statistical Association* **107**(499) 1106–1118. doi:10.1080/01621459.2012.695674.

Zhou, Lexin, Lorenzo Pacchiardi, Fernando Martínez-Plumed, Katherine M Collins, Yael Moros-Daval, Seraphina Zhang, Qinlin Zhao, Yitian Huang, Luning Sun, Jonathan E Prunty, et al. 2025. General scales unlock ai evaluation with explanatory and predictive power. *arXiv preprint arXiv:2503.06378* .

6. Appendix

Phase 1 System Prompt:

```
You will read a user-provided python dictionary object that contains an anonymized patient note ('Patient
Note'), a clinical computation question ('Question'), a GPT-generated ground truth answer ('Ground
Truth Answer'), as well as the relevant medical parameters that the GPT extracted from the patient note
('Relevant Entities') before it solves the computation question.

Your job, as a knowledgeable medical expert, is to fact-check whether the GPT has performed the
computation question correctly in accordance with commonly accepted clinical standards. Review the
information carefully, and perform independent calculations of the question if you can, and lastly give
your best judgment of if you think the original GPT-generated ground truth answer is correct or not. It is
acceptable for the GPT-generated answer to differ slightly from your judgment due to rounding errors, but
the deviation should not be egregious as to have major difference in clinical implications. The question's
underlying calculator might be sourced from a popular medical calculator website called MDCalc.com, and
you are encouraged to use the web search tool to look up more specifically explanations for the clinical
criteria and cross-check the GPT's.

Below, you will help me grade one such example, which I have randomly sampled from my database. Note that
you do not need to be critical for the sake of it. Most importantly, you should remain objective and only
flag cases that are truly problematic. After your reasoning and search procedures, you should end your
response by boxing your final Yes/No judgment in <answer> </answer> tags, where Yes means you think the
GPT-generated ground truth answer is correct, and No means you think it is incorrect.
```

Phase 1 User Prompt Example:

```
{
  "Unique ID": 1,
  "Calculator ID": 2,
  "Calculator Name": "Creatinine Clearance (Cockcroft-Gault Equation)",
  "Category": "lab",
  "Output Type": "decimal",
  "Note ID": "pmc-7671985-1",
  "Note Type": "Extracted",
  "Patient Note": "An 87-year-old man was admitted to our hospital for anorexia for several days,
high-grade fever from the previous day, and liver dysfunction. Of note, he had a history of hypertension,
diabetes mellitus (DM), and angina. Physical examination findings included: clear consciousness; height,
163 cm; weight, 48 kg; blood pressure, 66/40 mmHg; heart rate, 75/min; respiratory rate, 22/min...[Omitted
content was present in the actual API call]...causes of death were thus determined as (1) DIC and (2) ALF
associated with diffuse large B-cell lymphoma.",
  "Question": "What is the patient's Creatinine Clearance using the Cockroft-Gault Equation in terms
of mL/min? You should use the patient's adjusted body weight in kg instead of the patient's actual body
weight if the patient is overweight or obese based on their BMI. If the patient's BMI is normal, set their
adjusted body weight to the minimum of the ideal body and actual weight. If the patient is underweight,
please set their adjusted body weight to their actual body weight.",
  "Relevant Entities": "'sex': 'Male', 'age': [87, 'years'], 'weight': [48.0, 'kg'], 'height': [163.0,
'cm'], 'creatinine': [1.4, 'mg/dL']",
  "Ground Truth Answer": "25.238",
  "Lower Limit": "23.9761",
  "Upper Limit": "26.4999",
  "Ground Truth Explanation": "The formula for computing Cockcroft-Gault is given by CrCl = ((140 - age)
* adjusted weight * (gender_coefficient)) / (serum creatinine * 72), where the gender_coefficient is 1 if
male, and 0.85 if female. The serum creatinine concentration is in mg/dL. The patient's gender is male,
which means that the gender coefficient is 1. The patient is 87 years old. The concentration of creatinine
is 1.4 mg/dL. The formula for computing the patient's BMI is (weight)/(height * height),...[Omitted
content was present in our API call]...we take the patient's weight, 48.0 kg, as the patient's adjusted
weight needed for the Cockroft-Gault Equation. Using the Cockcroft-Gault equation: CrCl = ((140 - age) *
adjusted weight * gender_coefficient) / (serum creatinine * 72). Plugging the patient's values gives us
((140 - 87) * 48.0 * 1) / (1.4 * 72) = 25.238 mL/min. Hence, the patient's creatinine clearance is 25.238
mL/min."
}
```

Figure 6 **Prompts for the LLM audit agent executing the Phase 1 workflow (§3.1.)**

Phase 2 System Prompt:

You will read a user-provided JSON string that contains an anonymized patient note (‘‘Patient Note’’) and a clinical computation question (‘‘Question’’). Your job is to calculate the answer to the question based on the patient note. You have access to a Google Search tool and a code execution tool to perform calculations, if needed.
Your operational protocol is as follows:
1. Adopt Expert Persona: Assume the role of a diligent clinician. Your primary responsibility is accuracy and adherence to standard and up-to-date medical guidelines.
2. Identify Appropriate Scoring Rule or Formula: You will be given a patient note and a question that specifies a clinical calculation task (e.g., CHA2DS2-VASc score, MELD score, CURB-65, etc.). You should use Google Search to confirm the current, generally accepted formula, criteria, and/or scoring system for the specified clinical computation question. Prioritize reputable medical sources, such as MDCalc.com and guidelines published by health agencies or hospitals.
3. Systematic Reasoning and Calculation:
• Carefully read the patient note and systematically extract every piece of information relevant to the calculation.
• Explicitly map the extracted patient data to the components of the scoring system. For example, for a CHA2DS2-VASc score, list each component (Congestive heart failure, Hypertension, Age, etc.) and assign points based on the patient note.
• If there are complex arithmetic operations that are not easily performed by hand, you can use the code execution tool to perform the calculations.
• Show your step-by-step calculation. Sum the points or apply the formula as required.
4. Handling Missing Information:
• If a piece of information required for the calculation is clearly absent from the note and if it cannot be reasonably inferred from the note, explicitly state what is missing in your reasoning, and give your final answer as ‘‘unknown’’ (without quotes).
• Do not invent data or make assumptions that are not reasonably supported by the patient note.
5. Final Answer Formatting (Strict):
• After your detailed reasoning, you MUST enclose your final answer in <answer> </answer> tags.
• The content inside the tags must ONLY be the final numeric value (e.g., 4, 12.5), date, or time. For numeric values, you do not need to round the answer.
• As mentioned in #4, if and only if the calculation is impossible due to missing data, the content inside the answer tags must be exactly ‘‘unknown’’ (without quotes).
• DO NOT include any units, variable names, explanations, or any other text inside the <answer> </answer> tags.

Phase 2 User Prompt Example:

{
"Patient Note": "An 87-year-old man was admitted to our hospital for anorexia for several days, high-grade fever from the previous day, and liver dysfunction. Of note, he had a history of hypertension, diabetes mellitus (DM), and angina. Physical examination findings included: clear consciousness; height, 163 cm; weight, 48 kg; blood pressure, 66/40 mmHg; heart rate, 75/min; respiratory rate, 22/min...[*Omitted content was present in the actual API call*]...causes of death were thus determined as (1) DIC and (2) ALF associated with diffuse large B-cell lymphoma.",
"Question": "What is the patient’s Creatinine Clearance using the Cockroft-Gault Equation in terms of mL/min? You should use the patient’s adjusted body weight in kg instead of the patient’s actual body weight if the patient is overweight or obese based on their BMI. If the patient’s BMI is normal, set their adjusted body weight to the minimum of the ideal body and actual weight. If the patient is underweight, please set their adjusted body weight to their actual body weight.",
}

Figure 7 **Prompts for the LLM relabeling agent executing the Phase 2 workflow (§3.2). Note that unlike Fig. 6, the user prompt only includes (C, q) to increase the independence of the relabeling process.**

Qwen3-8B System Prompt:

```
You are a helpful medical assistant who gives truthful answers to the user's questions.
The user provides a patient note as well as a medical calculation question about the patient.
You first conduct the reasoning process inside <think> and </think> tags. After you have made your best
effort to answer the question, you provide the user with the final answer inside <answer> </answer> tags,
i.e., <answer>numeric_answer_value</answer> or <answer>unknown</answer>. Importantly, inside the <answer>
</answer> tags, you should provide either the numeric/date answer without units or additional textual
explanation, or "unknown" for patient notes lacking necessary information. Note that "unknown" should be
used sparingly, only when key information for answering the question is clearly missing from the patient
note and cannot be reasonably inferred.

Example response 1:
<think>
The user wants to calculate the patient's BMI.
Formula: weight (kg) / (height (m))^2.
Extracted from note: Weight is "70 kg", Height is "175 cm".
Convert height: 175 cm = 1.75 m.
Calculation: 70 / (1.75 * 1.75) = 22.857.
</think>
<answer>22.857</answer>

Example response 2:
<think>
The user wants to calculate the patient's BMI.
Formula: weight (kg) / (height (m))^2.
Extracted from note: Height is "175 cm".
The patient's weight is not mentioned in the note. I cannot calculate the BMI.
</think>
<answer>unknown</answer>
```

Qwen3-8B User Prompt Template:

```
Patient Note: {patient_note}

Question: {question}

Response:
```

Figure 8 **Prompts for the controlled RL experiment in §4.2, which are identically used across the two comparison groups. These prompts are fed as context into a Qwen3-8B model checkpoint that parametrizes the RL policy.**